

**UNIVERSITY OF BUCHAREST  
FACULTY OF CHEMISTRY  
DOCTORAL SCHOOL OF CHEMISTRY**

**ABSTRACT OF THE PhD THESIS**

**NEW BIOSENSORS BASED ON A  
RATIONAL DESIGN OF THE BIOMOLECULE-  
TRANSDUCER INTERFACE**

**PhD student,  
Lucian-Gabriel Zamfir**

**PhD supervisor,  
Prof. dr. Camelia Bala**

## TABLE OF CONTENTS

(The numbering of the pages is the one from the PhD thesis)

INTRODUCTION	8
THEORETICAL PART	10
1 Biosensors	11
1.1 Enzymatic biosensors	13
1.1.1 Enzymatic biosensors based on cholinesterases	16
1.1.1.1 The biochemical role of cholinesterases	16
1.1.1.2 The mechanism of inhibition of acetylcholinesterase	17
1.1.1.3 Biosensors for the detection of acetylcholinesterase inhibitors	19
1.2 Immunosensors	23
1.2.1 Electrochemical immunosensors	24
1.2.2 SPR immunosensors	24
2 The design of the biomolecule-transducer interface	27
2.1 The interface modified with magnetic beads	27
2.2 The interface modified with gels based on ionic liquids	28
3 The compounds of interest	31
3.1 Mycotoxins	31
3.2 Organophosphates	34
3.3 Carbamate drugs	36
4 References	39
EXPERIMENTAL PART	52
5 Immunosensors based on magnetic beads	53
5.1 The working principle of the immunosensor	53
5.2 Materials and reagents	53
5.3 Equipments	54
5.4 The preparation of the immunosensor	55
5.4.1 The immobilization of antibodies for ochratoxin A on magnetic beads	55
5.4.2 The modification of the EIS gold electrode	56
5.4.3 The modification of the SPR gold chip	57
5.5 Results and discussions	58
5.5.1 The electrochemical characterization of the immunosensor	58
5.5.1.1 Cyclic voltammetry	58
5.5.1.2 Electrochemical impedance spectroscopy	59
5.5.2 The characterization of the immunosensor using SPR	61
5.5.3 The detection of ochratoxin A using electrochemical impedance spectroscopy	61
5.5.4 The detection of ochratoxin A using a SPR immunosensor	63
5.6 Conclusions	64
5.7 References	66
6 Biosensors with acetylcholinesterase based on composite materials	67
6.1 The detection of organophosphate pesticides	67
6.2 The determination of the acetylcholinesterase activity	68
6.3 The immobilization of acetylcholinesterase	71
6.4 Carbon paste sensors for thiocholine modified with IL-MWCNT gels	73
6.4.1 Materials and reagents	73
6.4.2 Equipments	75
6.4.3 The preparation of the MWCNT/CP, IL-MWCNT/CP and IL/CP sensors	75
6.4.3.1 The preparation of the IL-MWCNT composite gel	76
6.4.3.2 The preparation of the CP, MWCNT/CP, IL-MWCNT/CP and IL/CP sensors	78
6.4.4 Results and discussions	79
6.4.4.1 Cyclic voltammetry studies	79
6.4.4.2 The effect of pH on the thiocholine oxidation potential	89
6.4.4.3 Electrochemical impedance spectroscopy studies	91
6.4.4.4 Chronoamperometric measurements	92

6.5	Carbon paste biosensors based on IL-MWCNT gels	94
6.5.1	Results and discussions	95
6.5.1.1	The optimization of the storage conditions for the biosensors	95
6.5.1.2	The optimization of the quantity of immobilized acetylcholinesterase	96
6.5.1.3	Study on the effect of the IL on the immobilized acetylcholinesterase	98
6.5.1.4	The detection of chlorpyrifos	100
6.5.1.5	The biosensor regeneration	101
6.5.2	Conclusions	106
6.5.3	References	108
6.6	Screen-printed biosensors modified with TCNQ-MWCNT composite mixtures	112
6.6.1	Introduction	112
6.6.2	Materials and reagents	113
6.6.3	Equipments	114
6.6.4	Results and discussion	114
6.6.4.1	The preparation of the MWCNT-TCNQ/SPE thiocholine sensors	114
6.6.4.2	The characterization of the composite mixtures using DR-UV-Vis and Raman spectroscopy	115
6.6.4.3	Cyclic voltammetry studies	117
6.6.4.4	Chronoamperometric studies	121
6.6.4.5	The characterization of the TCNQ-MWCNT/SPE sensors using electrochemical impedance spectroscopy	123
6.6.4.6	Differential pulse voltammetry and amperometric studies	124
6.6.4.7	The preparation of the AChE/MWCNT-TCNQ/SPE biosensors	126
6.6.4.8	The optimisation and characterization of the AChE/MWCNT-TCNQ/SPE biosensor	127
6.6.4.9	The detection of chlorpyrifos and methyl paraoxon	130
6.6.5	Conclusions	131
6.6.1	References	133
6.7	Carbon paste biosensors modified with TTF-TCNQ-IL gels	134
6.7.1	Materials and reagents	134
6.7.2	Equipments	135
6.7.3	Results and discussions	135
6.7.3.1	The preparation of the thiocholine sensors	135
6.7.3.2	The characterization of the gels using FT-IR spectroscopy and SEM	136
6.7.3.3	Cyclic voltammetry studies	137
6.7.3.4	Electrochemical impedance spectroscopy studies	141
6.7.3.5	Amperometric studies	143
6.7.3.6	The preparation of the AChE/TTF-TCNQ-IL/CP biosensor	144
6.7.3.7	The optimisation and characterization of the AChE/TTF-TCNQ-IL/CP biosensor	144
6.7.3.8	Application. Detection of neostigmine and eserine	145
6.7.4	Conclusions	147
6.7.5	References	149
7	GENERAL CONCLUSIONS	151
8	List of published works with the reported results	154

(The numbering of tables, figures and references is the one from the PhD thesis)

The PhD thesis is divided into two main parts: the THEORETICAL PART, which describes the data in the literature regarding the research topics addressed, and the EXPERIMENTAL PART, which presents the original contributions.

The first chapter presents general aspects concerning electrochemical biosensors based on enzymes and electrochemical and optic immunosensors. The second chapter discusses the methods of modification of the biomolecule-transducer interface using magnetic beads or different composite materials based on carbon nanotubes, ionic liquids and redox mediators. The third chapter describes the compound of interest: ochratoxin A, organophosphate pesticides and carbamate drugs.

The experimental part presents the development, characterization and establishing of the performance parameters for: impedimetric and SPR immunosensors for ochratoxin A modified with magnetic beads, electrochemical sensors for thiocholine modified with different composite materials (IL-MWCNT, MWCNT-TCNQ and TTF-TCNQ-IL) and the corresponding biosensors, used in the detection of organophosphate and carbamate compounds.

The main objective of this thesis is the modification of the biomolecule-transducer interface of a biosensor, with different materials, simple or composite, which lead to a significant improvement of the response characteristics.

The development of the biosensors takes into account the choosing of the bioreceptor (antibody or enzyme) suitable for the analyte, the principles regarding the preparation of the biosensor, the planning of the biomolecule-transducer interface design, the preparation and the characterization of the modified biosensors and the detection of the compounds.

The application of the rational design concept in the development of biosensors modified with composite materials is represented by the selection of precursors for the composite materials which through their synergistic effect lead to the achievement of performance characteristics superior to those given by the precursors.

The first application described in the experimental part is represented by the use of functionalized magnetic beads for the development of ochratoxin A (OTA) immunosensors. The magnetic beads (PM) were used as support for the binding of OTA-specific antibodies and the preparation of impedimetric and optic immunosensors. The next applications describe the use of multiwalled carbon nanotubes (MWCNT), ionic liquids with imidazolium cations (IL) and electrochemical mediators (TTF, TCNQ) for the preparation of composite mixtures. The prepared materials, IL-MWCNT, MWCNT-TCNQ and TTF-TCNQ-IL, were used in the development of electrochemical sensors for thiocholine (TCh) detection. The TCh sensors were used in the development of biosensors based on the inhibition of acetylcholinesterase (AChE) for the detection of inhibitor compounds.

## **5 IMMUNOSENSORS MODIFIED WITH MAGNETIC BEADS**

Magnetic beads allow the immobilization of a large number of antibodies (Ac) on the surface of a sensor and their easy manipulation using a magnet. The immobilization method used in the preparation of an OTA immunosensor relied on the binding of OTA-specific antibodies on the surface of PM modified with carboxylic groups. The detection of OTA is the result of the antigen-antibody affinity interaction which leads to a variation of the resistance measured by an

impedimetric immunosensor. The resulting immunosensor doesn't need a marker and can be reused.

The immobilization of anti-OTA antibodies on the PM is based on the covalent binding between the carboxyl groups of the PM and the amino ones of the Ac. In order to activate the carboxyl groups on the PM, a carbodiimide, EDC, was used. The modification of the gold electrode has several steps, presented in M in Fig. 0-1. On a cleaned gold electrode, a layer of thiols is immobilized, on which glutaraldehyde and then BSA are deposited. A gold electrode modified with BSA is obtained. On the surface of a cleaned gold electrode, a thiolic layer is deposited, followed by glutaraldehyde and then BSA. On its surface, the Ac-PMs are attached, thus obtaining the OTA immunosensor.

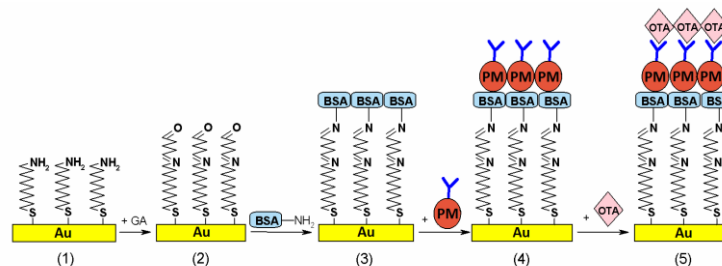


Fig. 0-1. The preparation steps for the EIS immunosensor: (1) Au/TA; (2) Au/TA/GA; (3) Au/TA/GA/BSA; (4) immunosensor OTA Au/TA/GA/BSA/Ac-PM; (5) the detection of OTA.

Cyclic voltammetry was used to characterize each step of the preparation of the immunosensor, in a potential range of  $-700 \div +700$  mV (vs SCE), at a scan rate of 100 mV/s, in the presence of a 2.5 mM  $K_3[Fe(CN)_6]/K_4[Fe(CN)_6]$  solution (1:1).

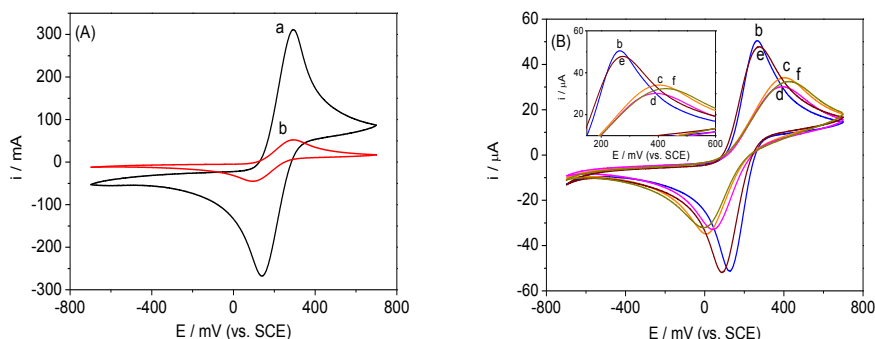


Fig.5-4. Cyclic voltammetry measurements in the presence of 2.5 mM  $K_3[Fe(CN)_6]/K_4[Fe(CN)_6]$  for the electrode: (A) Au (a) Au; (b) Au/TA; (B). (c) Au/TA/GA; (d) Au/TA/GA/BSA; (e) Au/TA/GA/BSA/Ac-PM -the immunosensors; (f) immunosensor + 0.1 ng/mL OTA. ( $v_s = 100$  mV/s)

The voltammogram registered for the gold electrode shows two reversible peaks which shows the absence of impurities (Fig. 5-4.A., curve a), and those registered for SAM-modified surface showed a blocking effect of the SAM on the electron transfer. The interaction between a sample of OTA and the Ac-PM layer was followed by a decrease of the faradaic response and an increase of the separation between the anodic and cathodic potential values (Fig. 5-4., curve f), from which suggests that the charge transfer between  $Fe(CN)_6^{4-}/Fe(CN)_6^{3-}$  and the electrode surface is inhibited.

In the electrochemical impedance spectroscopy studies the variation of the charge transfer resistance on the electrode surface was monitored. Fig. 5-5. presents the Nyquist plots for the

unmodified gold electrode and for those modified after each immobilization stage, registered in a  $\text{Fe}(\text{CN})_6^{4-}/\text{Fe}(\text{CN})_6^{3-}$  solution.

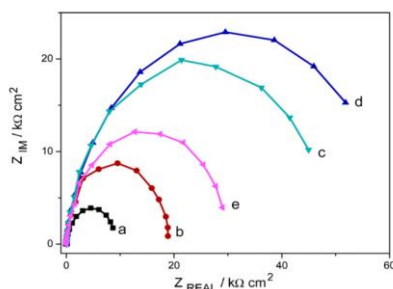


Fig.5-5. Nyquist diagrams ( $Z_{\text{REAL}}$  vs.  $Z_{\text{IM}}$ ) of the impedance measurements for the electrodes: (a) Au; (b) Au/TA; (c) Au/TA/GA; (d) Au/TA/GA/BSA; (e) Au/TA/GA/BSA/Ac-PM

After the deposition of the BSA, the value of the resistance increased considerably due to the formation of a negatively charged layer which act as an electrostatic barrier between the electrode surface and the  $\text{Fe}(\text{CN})_6^{4-}/\text{Fe}(\text{CN})_6^{3-}$  anions in the solution. For the Au/TA/GA/BSA electrode no change of the signal was observed after adding solutions of OTA of different concentrations, which shows that between OTA and the electrode surface there are no adsorption phenomena or other non-specific interactions.

The affinity interaction between the antibody and the antigen lead to an increase of the resistance which is correlated with the increase of the semicircle diameter registered in EIS for the tested solutions. The increase in charge transfer resistance, proportional to the decimal logarithm of the OTA concentration, is explained by the fact that the OTA molecules bound to the immobilized antibodies offer a surplus of negative charges. The OTA molecule has a carboxylic group and a phenolic one which offer the OTA molecule two anionic forms: a monoanion ( $\text{OTA}^-$ ) and a dianion ( $\text{OTA}^{2-}$ ). The corresponding Nyquist diagrams are presented in Fig. 5-7.A, and the calibration curve presented in Fig. 5-7.B shows a non-linear dependence of the charge transfer resistance ( $\Delta R_2$ ) toward the logarithm of the OTA concentration. The linear range of the impedimetric immunosensor is 0.01-5 ng/mL OTA. The impedimetric immunosensor shows a sensitivity of 26.83 k $\Omega$  per decade, with a  $R^2 = 0.9676$  and a detection limit of 0.01 ng/mL OTA. A relative standard deviation of 4.7% was calculated for five repeated measurements, carried out for the same OTA concentration.

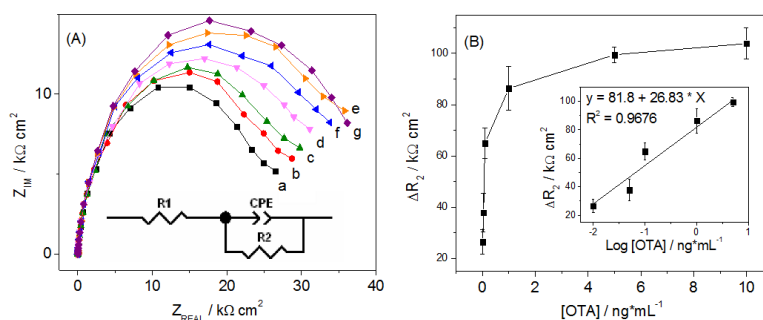


Fig.5-7. (A) Nyquist diagrams obtained after the incubation of the immunosensor in OTA solutions: (a) 0 ng/mL; (b) 0.01 ng/mL; (c) 0.05 ng/mL; (d) 0.1 ng/mL; (e) 1 ng/mL; (f) 5 ng/mL; (g) 10 ng/mL (2.5 mM  $\text{K}_3[\text{Fe}(\text{CN})_6]/\text{K}_4[\text{Fe}(\text{CN})_6]$ ,  $E = -400$  mV vs. SCE,  $\nu = 100$  mHz - 100 kHz). (B) The calibration curve of the immunosensor ( $\Delta R_2$ ) for OTA concentrations between 0.01 and 10 ng/mL ( $n = 5$ ); inset: calibration curve of the EIS immunosensor.

The measurements with the SPR immunosensors were carried out in the 0.1-100 ng/mL OTA concentration range. An increase of the resonance angle was observed, proportional to the OTA concentration, which is a result of the affinity interactions between OTA and the immobilized antibodies. For the solution with concentrations of OTA in the 1-50 ng/mL range a  $\Delta\theta = f([\text{OTA}])$  linear dependence was obtained with a  $R^2 = 0.9899$ .

The EIS immunosensor was tested in white wine samples spiked with 0.1, 0.5, 1, 2 and 5 ng/mL OTA, and the SPR immunosensor was tested using 1, 2, and 5 ng/mL OTA. The results were compared with those obtained ELISA kits (Ridascreen kit for OTA), as reference method.

The strategy used in the development of the OTA immunosensor takes into account the need to regenerate the surface of the immunosensor and so the immobilization of OTA specific antibodies on PM was chosen. The immobilization of the Ac-PM on the gold surface is carried out using a magnet. The non-specific interactions between OTA and the gold surface have been eliminated by using a layer of BSA on the gold electrode, increasing the specificity of the immunosensor. The use of PM allowed an easy immobilization of the antibody and doesn't require the use of a marker.

### Selective Bibliography

- [3] J.J. Monagle, Carbodiimides. III. Conversion of Isocyanates to Carbodiimides. *Catalyst Studies, The Journal of Organic Chemistry*, 27 (1962) 3851-3855.
- [5] P.R. Perrotta, N.R. Vettorazzi, F.J. Arévalo, A.M. Granero, S.N. Chulze, M.A. Zón, H. Fernández, Electrochemical studies of ochratoxin a mycotoxin at gold electrodes modified with cysteamine self-assembled monolayers. Its ultrasensitive quantification in red wine samples, *Electroanalysis*, 23 (2011) 1585-1592.
- [14] J. Wu, H. Chu, Z. Mei, Y. Deng, F. Xue, L. Zheng, W. Chen, Ultrasensitive one-step rapid detection of ochratoxin A by the folding-based electrochemical aptasensor, *Analytica Chimica Acta*, 753 (2012) 27-31.
- [15] X.H. Fu, Surface plasmon resonance immunoassay for ochratoxin a based on nanogold hollow balls with dendritic surface, *Analytical Letters*, 40 (2007) 2641-2652.

## 6 BIOSENSORS WITH ACETYLCHOLINESTERASE BASED ON COMPOSITE MATERIALS

The inhibition of AChE by different species is the basis for the development of biosensors for inhibitor detection. A decrease of the enzymatic activity occurs as a result of the interaction between an inhibiting compound and AChE. The inhibition degree of AChE is calculated by measuring the enzymatic activity before and after incubating in a solution containing the inhibitor, and it is calculated using formula 1-5.

$$I\% = \frac{A_0 - A_1}{A_0} \times 100$$

1-5. The formula for calculating the inhibition degree of an enzyme.

where:  $A_0$  = the initial enzymatic activity,  $A_1$  = the enzymatic activity after the incubation with the inhibitor and  $I\%$  = the inhibition degree.

In the case of inhibition-based biosensors, the linear range corresponds to a 20% ÷ 80% domain of the inhibition degree, and the detection limit is defined as the quantity of inhibitor that leads to a 10% inhibition percentage.

Due to the fact that the natural substrate for AChE, acetylcholine, doesn't generate an electroactive compound through hydrolysis, the amperometric biosensors based on AChE use a synthetic substrate, acetylthiocholine (ATCh). TCh is a compound with a thiol group that is formed from the enzymatic hydrolysis of ATCh and can be oxidized electrochemically to dithio-bis-thiocholine. The action of an inhibitor on the activity of AChE leads to a decrease of the enzymatic activity, and so to a decrease of the TCh concentration in the solution. The amperometric biosensor is immersed in a buffer and the corresponding signal ATCh is measured. The operating principle of the biosensor is presented in Fig. 6-1.

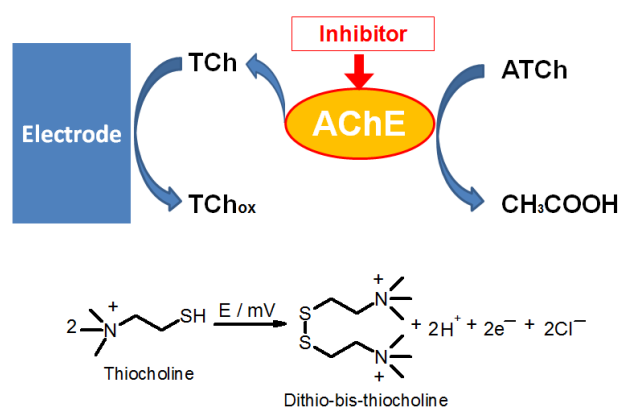


Fig. 6-1. The operating principle of the monoenzymatic biosensor.

The difference in current intensity for the enzymatically generated TCh registered before and after incubation in the pesticide solution, is used to calculate the inhibition degree corresponding to the concentration of inhibitor used.

The immobilization method used in all the experiments consists in the encapsulation of AChE in a sol-gel matrix. The porosity of the sol-gel matrix ensures the diffusion of the substrate molecules towards the catalytic site of the enzyme.

#### 6.4 Carbon paste sensors for thiocholine modified with IL-MWCNT gels

In this chapter of the experimental part the studies regarding the electrochemical properties of composite gels based on MWCNT and IL with imidazolium cation are presented. The electrochemical sensors for TCh developed in this experimental part are based on a carbon paste electrode modified with IL-MWCNT composite gels. The ionic liquids show high ionic conductivity and the ability to disperse carbon nanotubes. Between the two components  $\pi$ - $\pi$  and  $\pi$ -cation interaction are established which lead to the formation of a stable IL-CNT composite [16].

The preparation of the new types of gels based on IL and MWCNT is carried out by direct mixing and the use of ultrasounds to facilitate the dispersion of the MWCNT in the IL. The ionic liquids used in the electrochemical experiments have an imidazolium based cation and different organic and inorganic anions. The study of the influence of the ionic liquid structure on the electrochemical properties was taken into account when choosing the ionic liquids. The rational design consists in the selection of precursors for the composite materials which can lead, through



a synergistic effect, to the obtaining of properties superior to those of the individual components. What was pursued was the combining of the properties of MWCNTs, such as mechanic resistance and electric conductivity, with those of IL, such as ionic conductivity and the ability to disperse MWCNT. These are the first experiments reported concerning the use of IL-MWCNT for the detection of TCh.

The CP, MWCNT/CP, IL-MWCNT/CP and IL/CP sensors were characterized using cyclic voltammetry, in a  $-400 \div 800$  mV potential range, with a scan rate of 100 mV/s. The results obtained with IL-MWCNT/CP were compared with those obtained with the sensors modified with the precursors in order to highlight the synergistic effect of the IL and MWCNT. For the cyclic voltammetry measurements in TCh, one of the aims of the sensor modification is the increase of the selectivity, by achieving low potential values for the oxidation of TCh, and the increase of the sensitivity by achieving higher values of the peak intensity for the oxidation of TCh. For the CP electrodes, the TCh oxidation peak has a potential value of +650 mV, and for the MWCNT-modified electrode the oxidation potential has a lower value, of +350 mV. This decrease of the oxidation potential, recorded for the MWCNT/CP sensor (Fig. 6-6.A.) can be assigned to the electrocatalytic properties and high electroactive surface of the MWCNTs.

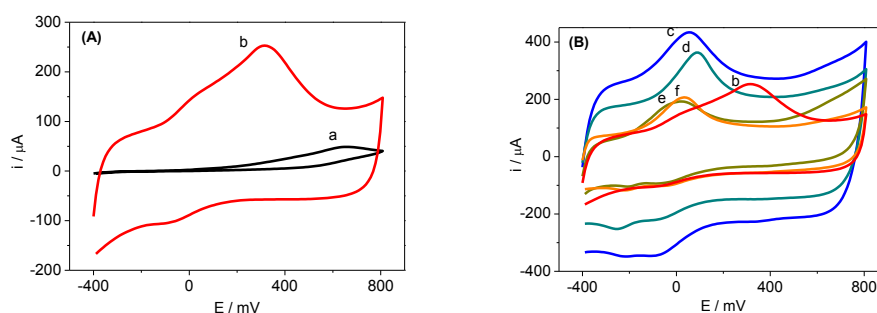


Fig.6-6. Cyclic voltammograms recorded in the presence of 5 mM TCh for the sensors: A) CP (a); MWCNT/CP (b); B) [BMIM][BF<sub>4</sub>]-MWCNT/CP (c); [EMIM][NTF<sub>2</sub>]-MWCNT/CP (d); [EMIM][OTF]-MWCNT/CP (e) and [EMIM][TCB]-MWCNT/CP (f). ( $v_s = 100$  mV/s)

In the case of electrode modified with IL-MWCNT, the oxidation potential of TCh is at a lower value and the peak current intensity is higher. The voltammograms registered for the CP electrodes modified with [BMIM][BF<sub>4</sub>], [EMIM][NTF<sub>2</sub>], [EMIM][OTF] and [EMIM][TCB] gels are presented in Fig. 0-2.B. It was observed that the majority of the potential values for the IL-MWCNT/CP sensors are below +100 mV. The low values of the oxidation peak for TCh registered for the IL-MWCNT/CP sensors are due to the fact that the gel can accelerate the electron transfer because of the electrostatic interactions between the TCh molecules, negatively charged at pH = 8 and the imidazolium cation of the IL. It was observed that for the sensors with four gels the values of the sensitivity were higher than that of MWCNT/CP, the highest being recorded for [BMIM][BF<sub>4</sub>]-MWCNT.

Although the MWCNT shows a sensitivity value almost twice as large compared to that of the CP sensors, the gels show higher values, the [BMIM][BF<sub>4</sub>]-MWCNT/CP electrode having the highest one. Sensors modified with gels based on [HMIM][PF<sub>6</sub>], [EMIM][NTF<sub>2</sub>], [EMIM][PF<sub>6</sub>] and [EMIM][FAP] have shown low sensitivity values for TCh. Because the [BMIM][BF<sub>4</sub>]-MWCNT gel showed the highest current value for the oxidation of TCh and a low potential, it was chosen for the next experiments.

## 6.5 Carbon paste biosensors modified with IL-MWCNT gels

For the ATCh amperometric measurements the calibrations were carried out by successive additions in the 0.1-10 mM ATCh concentration domain. The detection of ATCh was carried out in amperometry at a +50 mV potential by successive additions of ATCh in a PBS solution with 1 UI AChE.

Amperometric measurements were carried out for different values of the enzymatic activity of the immobilized enzyme, in 5 mM ATCh, before and after incubation with the chlorpyrifos pesticide. The optimal quantity of AChE was determined through measurements of the inhibition percentage by incubating in chlorpyrifos solution with concentrations between  $10^{-8}$  and  $10^{-6}$  M. The value of the inhibition degree of AChE was calculated for each concentration and the values are presented in Fig. 6-17.

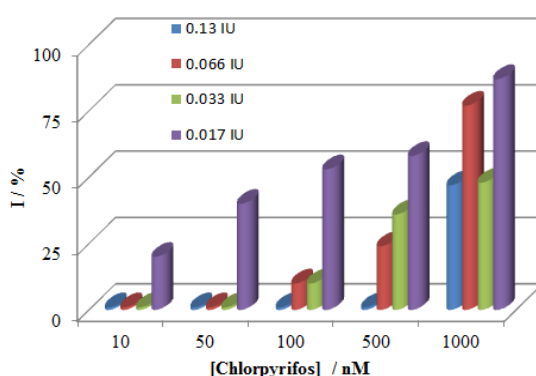


Fig.6-17. The effect of the enzyme quantity on the inhibition degree of the biosensor AChE/[BMIM][BF<sub>4</sub>]-MWCNT/CP (AChE 17-130 mUI, E = +50 mV, [ATCh] = 5 mM, pH = 8, T<sub>incubation</sub> = 15 min.).

The results show that an enzymatic activity of 17 mIU is the optimal value for chlorpyrifos measurements based on the inhibition of AChE because for this value inhibition was registered for  $10^{-8}$  M and  $5 \times 10^{-8}$  M chlorpyrifos. Chlorpyrifos measurements were carried out using the AChE/[BMIM][BF<sub>4</sub>]-MWCNT/CP biosensor, in the  $10^{-8} \div 10^{-6}$  M concentration range. The amperometric signal was recorded for a potential value of +50 mV, in the presence of 5 mM ATCh. Measurements for the optimization of the incubation time were carried out for a solution of  $10^{-8}$  M chlorpyrifos, ranging from 5 to 30 minutes, and the optimal incubation time is 15 minutes, a value reported by other authors [57].

The calibration curve shown in Fig. 6-19. is a  $I\% = \text{Log}[\text{Chlorpyrifos}]$  semi logarithmic representation. The detection limit calculated for 10 % inhibition degree is 4 nM chlorpyrifos (1.4 ppb).

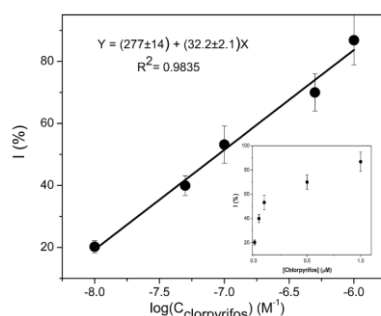


Fig.6-19. The calibration curve  $I\% = \text{Log}[\text{Chlorpyrifos}]$  for chlorpyrifos (inset:  $I\% = [\text{Chlorpyrifos}]$ ). (AChE 17 mIU, E = +50 mV, [ATCh] = 5 mM, pH = 8, n = 5).

Another objective is represented by the regeneration the biosensor surface. Organophosphate pesticides inhibit AChE irreversibly, and it can be regenerated by oxime reagents such as PAM and obidoxime. The regeneration compounds react with the inhibitor which is covalently bound with the enzyme and removes it from the active site. The mechanism of the action of obidoxime on the AChE inhibited by chlorpyrifos is presented in Fig. 6-16.

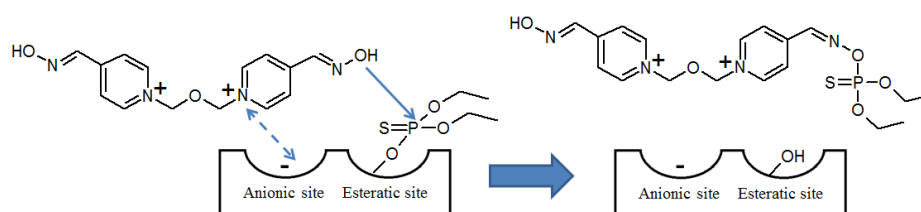


Fig.6-12. The principle of the regeneration of chlorpyrifos inhibited AChE using obidoxime.

The regeneration potency of obidoxime was studied for a concentration of 10 nM chlorpyrifos. The initial inhibition percentage is 20%. The biosensor was immersed in a stirred obidoxime solution. It was observed that a period of 5 minutes is sufficient for a total reactivation of the enzymatic activity. A concentration of 0.1 mM obidoxime is considered to be optimal for the regeneration of the enzyme.

The regeneration studies carried out with obidoxime and PAM on identical biosensor in the same solution of chlorpyrifos have shown that obidoxime is a more efficient reactivation reagent of AChE compared to PAM. For all the next experiments which involve AChE inhibitors obidoxime was used as the reactivation reagent.

In this chapter the design of a TCh sensor based of IL-MWCNT was described. The sensor [BMIM][BF<sub>4</sub>]-MWCNT/CP, characterized by an increased sensitivity and a low potential for the oxidation of TCh, was used in the development of a biosensor for organophosphate compounds based on AChE. The quantity of immobilized enzyme on the [BMIM][BF<sub>4</sub>]-MWCNT/CP sensors was optimized in order to record a high inhibition degree for a low concentration of chlorpyrifos. A detection limit of 4 nM for chlorpyrifos was calculated for a biosensor with 17 mIU AChE. In this thesis the use of obidoxime for the regeneration of AChE immobilized on a biosensor was reported for the first time.

### Selective references

- [14] S. Andreescu, L. Barthelmebs, J.L. Marty, Immobilization of acetylcholinesterase on screen-printed electrodes: comparative study between three immobilization methods and applications to the detection of organophosphorus insecticides, *Analytica Chimica Acta*, 464 (2002) 171-180.
- [16] T. Fukushima, A. Kosaka, Y. Ishimura, T. Yamamoto, T. Takigawa, N. Ishii, T. Aida, Molecular ordering of organic molten salts triggered by single-walled carbon nanotubes, *Science*, 300 (2003) 2072-2074.
- [27] R.T. Kachoosangi, M.M. Musameh, I. Abu-Yousef, J.M. Yousef, S.M. Kanan, L. Xiao, S.G. Davies, A. Russell, R.G. Compton, Carbon nanotube-ionic liquid composite sensors and biosensors, *Anal Chem*, 81 (2009) 435-442.
- [29] B.G. Choi, H. Park, T.J. Park, D.H. Kim, S.Y. Lee, W.H. Hong, Development of the electrochemical biosensor for organophosphate chemicals using CNT/ionic liquid bucky gel electrode, *Electrochemistry Communications*, 11 (2009) 672-675.

[57] D. Du, X. Ye, J. Cai, J. Liu, A. Zhang, Acetylcholinesterase biosensor design based on carbon nanotube-encapsulated polypyrrole and polyaniline copolymer for amperometric detection of organophosphates, *Biosensors and Bioelectronics*, 25 (2010) 2503-2508.

## 6.5 Screen-printed biosensors modified with TCNQ-MWCNT composite mixtures

One of the most widely used mediators in the development of sensors and biosensors is 7,7,8,8-tetracyanoquinodimethane, an organic molecule which is an electron acceptor and has electrocatalytic properties [1]. Until now the use of the MWCNT and TCNQ mixtures for modifying TCh sensors has not been reported. Three types of screen-printed electrodes were prepared, each modified with a different material: electrodes modified with MWCNT (MWCNT/SPE), with TCNQ (TCNQ/SPE) and those modified with the MWCNT-TCNQ (MWCNT-TCNQ/SPE) composite.

The MWCNT-TCNQ composite was characterized using DR-UV-Vis and Raman spectroscopy. The properties of this composite were compared to those of the precursors, MWCNT and TCNQ (Fig. 6-28.A).

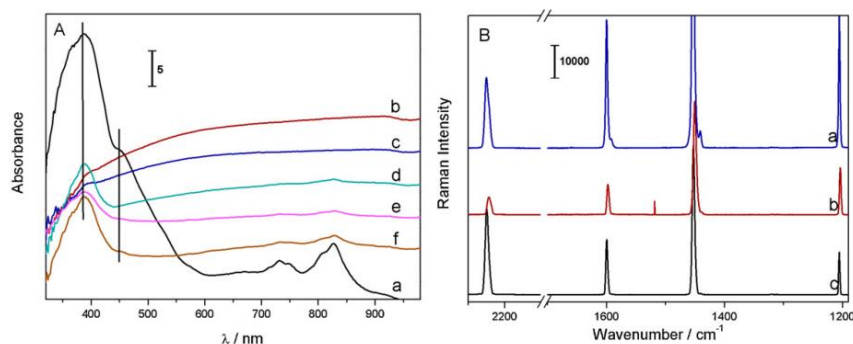


Fig. 6-28. A) The absorption spectra in DR-UV-Vis for TCNQ (a), MWCNT (b), MWCNT-TCNQ 1 mM (c), MWCNT-TCNQ 10 mM (d), MWCNT-TCNQ 100 mM (e), and MWCNT-TCNQ 200 mM (f). B) Raman spectra for TCNQ (a), MWCNT-TCNQ 100 mM (b) and MWCNT-TCNQ 200 mM (c).

For the DR-UV-Vis spectra of MWCNT-TCNQ 1 mM, the 454 nm band corresponding to the neutral molecule of TCNQ can no longer be seen which can be explained by the interactions between the CN groups of TCNQ and the aromatic rings of the carbon nanotubes. In the case of the Raman spectra (Fig. 6-28.B) for the MWCNT-TCNQ 100 mM a shift of the vibration band corresponding to the CN group can be seen, which is explained by an interaction between the CN groups and MWCNT. This shift no longer appears for MWCNT-TCNQ 200 mM, but shifts corresponding to the C=C can be observed and can be attributed to an electron transfer between the TCNQ anions [8]. The data obtained in the spectral analysis suggests the existence of two types of supramolecular organization depending on the concentration of TCNQ which are presented in Fig. 6-29: low concentrations of TCNQ (Fig. 6-29.A) and for high concentrations of TCNQ (Fig. 6-29.B).

For concentrations of TCNQ from 1 to 10 mM, the TCNQ molecules are arranged with the CN groups positioned towards the surface of the MWCNT as a result of the electrostatic interactions. For the MWCNT-TCNQ mixture with low mediator concentration, the TCNQ molecules have two functions: that of bridges between nanotubes, which are important in

stabilizing the composite mixture and to facilitate electron transfer between the nanotubes, and that of electron acceptors for the oxidation of TCh.

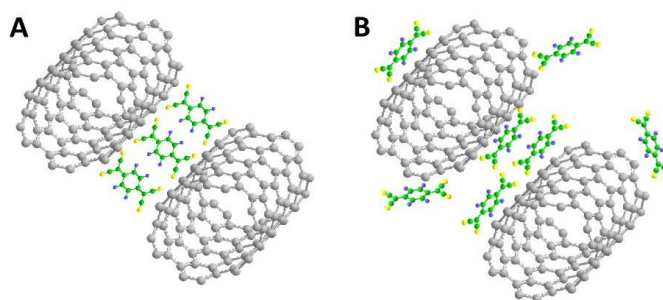


Fig. 6-19. Supramolecular organization of MWCNT-TCNQ at (A) low concentrations of TCNQ (<1 mM) and (B) high concentration of TCNQ (>10 mM).

Cyclic voltammetry studies were carried out with the following sensors: MWCNT/SPE, TCNQ/SPE and MWCNT-TCNQ/SPE. Fig. 6-31. shows the cyclic voltammograms registered in a mM TCh solution. It was observed that the oxidation potential of TCh has different values for each sensor used: +450 mV for MWCNT/SPE, +300 mV for TCNQ/SPE and +150 mV for MWCNT-TCNQ/SPE. A significant increase of the oxidation current was observed for the electrode modified with MWCNT-TCNQ compared to the other screen-printed electrode modified with TCNQ and MWCNT. The peak current intensity for the oxidation of TCh on MWCNT-TCNQ/SPE is 60  $\mu\text{A}$ , a value almost twice as high as that for MWCNT/SPE, and six times higher than that for TCNQ/SPE. This phenomenon is attributed to the synergistic effect of the two components, MWCNT and TCNQ.

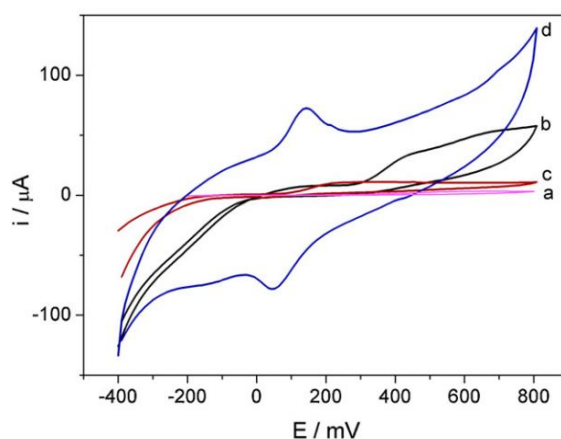


Fig. 6-13. Cyclic voltammograms registered for TCh 5 mM with SPE sensors (a), MWCNT/SPE (b), with TCNQ/SPE (c) and MWCNT-TCNQ/SPE (d) ( $v_s = 100 \text{ mV/s}$ ,  $[\text{TCNQ}] = 1 \text{ mM}$ ,  $\text{pH} = 8$ ).

Amperometric measurements of ATCh were carried out using the MWCNT-TCNQ/SPE and TCNQ/SPE electrodes, in a 10 mL cell with a magnetic stirrer. The calibration was made using the method of successive additions within a 0.1-5 mM ATCh concentration range. The current intensity for the baseline and the intensity of the signal for the enzymatically generated TCh were recorded. Between the measurements the sensors was rinsed with distilled water and phosphate buffer. A linear response was recorded for the 0.05-0.6 mM concentration range with a sensitivity of  $45 \mu\text{A}/\text{mM} \times \text{cm}^2$  and a detection limit of 30  $\mu\text{M}$  (Table 6-11.). For the electrode modified with TCNQ a lower sensitivity value of  $32 \mu\text{A}/\text{mM} \times \text{cm}^2$  was determined.

Table 6-10. The response parameters in amperometry for the TCNQ/SPE and MWCNT-TCNQ/SPE sensors ( $E = +150$  mV, pH = 8).

Sensor	Linear range mM	Slope $\mu\text{A} / \text{mM}$	Sensitivity $\mu\text{A} / \text{mM} \times \text{cm}^2$	$R^2$	$L_D$ $\mu\text{M}$
MWCNT-TCNQ	0.05-0.6	5.78	45.05	0.9785	28.5
TCNQ	0.05-0.4	4.02	32	0.9984	37.3

The AChE/MWCNT-TCNQ/SPE biosensor was used for ATCh measurements. The amperometric response was registered for successive additions of ATCh in a stirred solution of phosphate buffer at a working potential of +150 mV. The reproducibility of the analytic response for 5 mM ATCh was tested on 5 different biosensors, the % RSD being 6%. The amperometric response is at 96% of its initial value after one week, which suggest a good stability of the biosensor.

For the inhibition measurements two organophosphate pesticides were used, chlorpyrifos and methyl-paraoxonul. The calibration curves for methyl-paraoxon and chlorpyrifos were obtained for and incubation time of 30 minutes for each pesticide sample. Chlorpyrifos was determined in the  $10^{-8}$  -  $10^{-7}$  M concentration range, and methyl-paraoxonul in the  $10^{-9}$  -  $5 \times 10^{-7}$  M pesticide concentration range, with a similar reproducibility. The detection limits calculated for an inhibition degree of 10% are 30 pM (7 ppt) for methyl-paraoxon and 0.4 nM (0.1 ppb) for chlorpyrifos (Table 6-11.).

Table 6-11. The response characteristics for the AChE/MWCNT-TCNQ/SPE biosensor; equation  $I\% = a + b \times \log [\text{Pesticide}] (\text{M})$ . ( $T_{\text{incubation}} = 30$  min.)

Pesticide	a	b	$R^2$	Concentration range	Detection limit	
					pM	ppt
methyl- paraoxon	$195 \pm 12$	$17.6 \pm 1.3$	0.9722	0.1-500	30	7
chlorpyrifos	$258.2 \pm 5.6$	$26.50 \pm 0.70$	0.9958	1-100	430	100

The biosensor was used in pesticide detection in tap water samples. The inhibition degree registered in water (3.4 %) is smaller than the detection limit, which proves that the biosensor can be used in water samples without significant interference. Measurements were carried out in standard solutions and in tap water samples spiked with different quantities of methyl-paraoxon and chlorpyrifos. Solutions of 1, 10 and 50 mM methyl-paraoxon and 5, 10 and 50 mM chlorpyrifos were tested.

The experimental results obtained for real samples are presented in table 6-12 as inhibition percentages. The recovery was in all cases near 100 %.

Table 6-12. The detection of pesticides in water samples.

Pesticide	Pesticide concentration (nM)	Inhibition degree		Recovery %
		Standard solution	Spiked water sample	
methyl- paraoxon	1	37	$36 \pm 4$	97.3
	10	55	$52 \pm 5$	94.5
	50	67	$64 \pm 2$	95.5
chlorpyrifos	5	38	$33 \pm 2$	86.8
	10	46	$42 \pm 4$	91.3
	50	65	$61 \pm 3$	93.8

The formation of the MWCNT-TCNQ composite mixture based on MWCNT and the TCNQ mediator was confirmed by DR-UV-Vis and Raman measurements. The screen-printed electrodes modified with TCNQ, MWCNT and MWCNT-TCNQ were tested as sensors for TCh. Using the electrodes modified with MWCNT-TCNQ in cyclic voltammetry measurements has allowed a decrease of the oxidation potential of TCh from +450 mV for MWCNT/SPE to +150 mV for MWCNT-TCNQ/SPE. The sensitivity for TCh is almost six times higher for MWCNT-TCNQ/SPE than that for TCNQ/SPE. By using this composite a new amperometric biosensor for the detection of the pesticides methyl-paraoxon and chlorpyrifos was made based on the MWCNT-TCNQ/SPE electrode and AChE immobilized using the sol-gel method.

### Selective references

- [1] A. Ivanov, G. Evtugyn, H. Budnikov, F. Ricci, D. Moscone, G. Paleschi, Cholinesterase sensors based on screen-printed electrodes for detection of organophosphorus and carbamic pesticides, *Analytical and Bioanalytical Chemistry*, 377 (2003) 624-631.
- [6] J.P. McNamara, R. Sharma, M.A. Vincent, I.H. Hillier, C.A. Morgado, The non-covalent functionalisation of carbon nanotubes studied by density functional and semi-empirical molecular orbital methods including dispersion corrections, *Physical Chemistry Chemical Physics*, 10 (2008) 128-135.

### 6.7 Carbon paste biosensors modified with TTF-TCNQ-IL gels

This chapter of the experimental part describes the preparation of a new material made out of ionic liquids with imidazolium cations and the TTF-TCNQ charge-transfer complex. TTF and TCNQ are electrochemical mediators used in the development of sensors and biosensors. Within the charge-transfer complex TTF has the role of electron donor due to the conjugated  $\pi$  electrons, and TCNQ is an electron acceptor because of its four cyano groups. Mixing the two compounds results in the formation of TTF-TCNQ crystals which display high conductivity [1]. The literature describes the preparation and characterization of gels formed out of TTF, TCNQ and ILs with imidazolium cations [7]. The resulting materials are in the form of gels similar with the IL-CNT ones [8]. The observed synergistic effect is caused by the combination of the physical properties of the TTF-TCNQ complex with those of the IL, the obtained TTF-TCNQ-IL gel displaying both electric and ionic conductivity. The formation of the gel can be explained by the existence of electrostatic and  $\pi$ - $\pi$  between the TTF-TCNQ complex and the IL. Until now the literature has not reported the use of TTF-TCNQ-IL gels in the development of sensors and biosensors.

The formation of the TTF-TCNQ complex within the composite mixtures with IL was studied in FT-IR spectroscopy. Fig. 6-43 presents the spectra for TTF, TCNQ, [EMIM][TCB] and the TTF-TCNQ-[EMIM][TCB] gel. The shift of the vibration bands corresponding to the neutral TCNQ and TTF towards values that suggest the presence of the ionic forms for the TTF-TCNQ and TTF-TCNQ-[EMIM][TCB] mixtures can be explained through the formation of the charge-transfer complex.

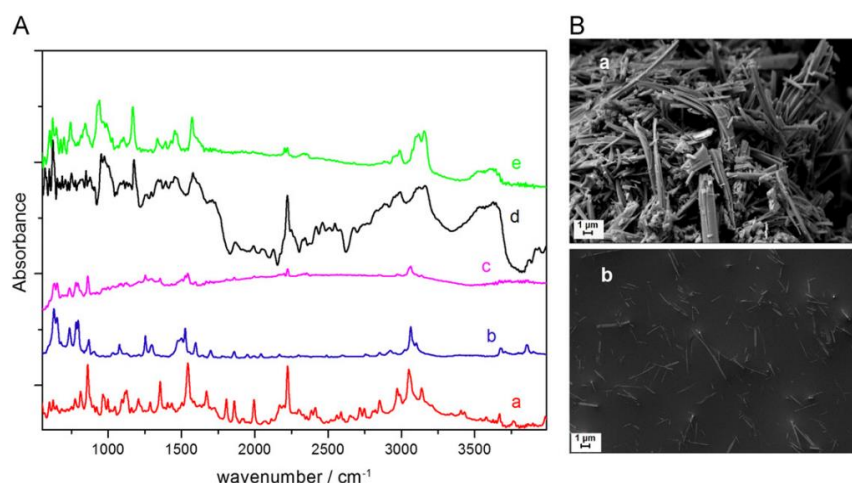


Fig.6-43. A) FT-IR spectra for: (a) TCNQ, (b) TTF, (c) TTF-TCNQ, (d) [EMIM][TCB], (e) TTF-TCNQ-[EMIM][TCB] gel. B) SEM images for (a) TTF-TCNQ, (b) TTF-TCNQ-[EMIM][TCB].

In the SEM images presented in Fig. 0-9.B, image a, the structure of TTF-TCNQ can be observed, which is made out of crystals arranged in the form of aggregates, and in image b, corresponding to the TTF-TCNQ-[EMIM][TCB] gel, the dispersion of these structures can be observed which indicates that [EMIM][TCB] behaves as an electrolyte towards the TTF<sup>+</sup> and TCNQ<sup>-</sup> ions within the TTF-TCNQ-[EMIM][TCB] gel.

Cyclic voltammetry studies using carbon paste sensors have allowed the comparison of the electrochemical properties of the composite materials with those of the precursors. Six types of sensors were tested: TCNQ/CP, TTF/CP, TTF-TCNQ/CP, IL/CP and TTF-TCNQ-IL/CP. The voltammograms recorded in 5 mM TCh are presented in Fig. 6-44. The electrochemical studies have shown a lower oxidation potential for TTF-TCNQ-[EMIM][TCB]/CP compared with the one registered for TTF-TCNQ/CP. The oxidation potential decreases +600 mV for TTF-TCNQ/CP to +395 mV for TTF-TCNQ-[EMIM][TCB]/CP, and the reduction potential decreases from -259 mV for TTF-TCNQ/CP to -143 mV for the gel-modified electrode. The increased electrocatalytic effect of the TTF-TCNQ-IL gels can be explained by the behaviour of the IL as a conductive matrix which allows the diffusion of the generated ions within the gel. The increased mobility of TTF<sup>+</sup> within the TTF-TCNQ-[EMIM][TCB] gel is due to the small volume of the TCB<sup>-</sup> anion.

The electrocatalytic properties of this gels can be explained by the high conductivity of [EMIM][TCB] compared to the other ionic liquids. For the [EMIM][TCB]-modified sensor a higher current for the oxidation of TCh was registered compared to the other modified electrodes, and for this reason it was used for the development of the enzymatic biosensor.

Amperometric measurements were carried out on the sensor modified with TTF-TCNQ-[EMIM][TCB] in TCh solutions with different concentrations, at a working potential of +400 mV vs. Ag/AgCl. A value of the  $k_{cat}$  of 32.3 L/mol×s was calculated, which shows an increased electrocatalytic effect of the TTF-TCNQ-[EMIM][TCB] towards the oxidation of TCh. This value is higher than that reported in the literature for an electrode modified with cobalt hexacyanoferrate [13], but it is lower than that reported for electrodes modified with IL-MWCNT or with TCNQ-MWCNT.



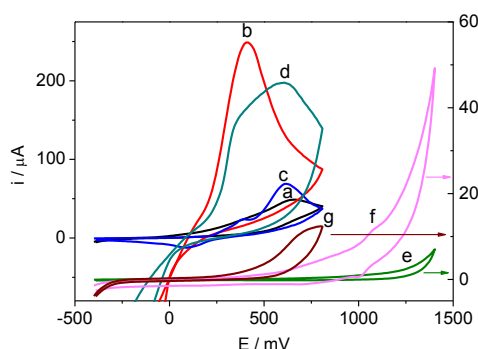


Fig.6-44. Cyclic voltammograms for : CP (a), TCNQ/CP (b), TTF/CP (c), TTF-TCNQ/CP (d), [EMIM][TCB]/CP (e)\*, [EMIM][NTF<sub>2</sub>]/CP (f)\* and [EMIM][OTF]/CP (g) \*, (\*The current is shown on the right axis)

The amperometric measurements with the AChE/TTF-TCNQ-IL/CP biosensors were carried out at a +400 mV working potential with successive additions of ATCh in PBS, in a 0.1-5 mM ATCh concentration range. For experiments carried out with the same biosensor the value of the RSD is 3.6% for 5 successive measurements in 5 mM ATCh. The operational stability was determined by carrying out five measurements in 5 mM ATCh for the same biosensor. The biosensors were stored at 4 °C. The signal keeps 92% of its initial intensity after two weeks.

The carbamate drugs used are eserine and neostigmine. Inhibition measurements were carried out for 10<sup>-6</sup> M eserine in order to optimize the incubation period. This was varied between 5 and 30 minutes and the inhibition degree increases with the incubation period from 5% to 100% for eserine. The calibration curves for eserine and neostigmine were obtained using a 30 minute incubation period. The response characteristics of the biosensor are presented in table 6-13. The detection limits are 26 pM (7 ppt) for eserine and 0.3 nM (57 ppt) for neostigmine, calculated for an inhibition degree of 10%. This is one of the lowest values reported in the literature.

Table 6-13. Response characteristics for AChE/TTF-TCNQ-IL/CP biosensor; the equation I% = a + b × log [Compound] (M). (T<sub>incubation</sub> = 30 min.)

Compound	a	b	R <sup>2</sup>	Concentration range (nM)	Detection limit	
					nM	ppt
eserine	220.4 ± 13.6	19.9 ± 1.7	0.9645	0.1-1000	0.03	7
neostigmine	247.2 ± 21.9	24.8 ± 2.8	0.9504	1-500	0.3	57

The achievement of low detection limits for the two carbamate compounds has allowed the use of biosensors based on AChE in waste water measurements. Measurements in real samples were carried out by adding known quantities of compound in tap water samples. The drug concentrations used were 10, 50 and 100 nM, and the experimental results are presented in table 6-14. Eserine and neostigmine were detected in the 0.1 - 1 nM concentration range.

The inhibition percentages obtained in real samples are correlated with the ones obtained for the standard solution. The recovery percentage of the two compounds was expressed as the ratio between the inhibition degree in the spiked water sample and that of the standard solution.

Table 6-14. The detection of carbamate compounds in water samples.

Compound	Concentration (nM)	Inhibition degree (%)		Recovery (%)
		Standard solution	Spiked water sample	
Eserine	10	61	54 ± 4	85.8
	50	75	70 ± 4	96.2
	100	81	94 ± 4	114.4
Neostigmine	10	49	38 ± 8	78
	50	66	65 ± 1	97.8
	100	74	76 ± 4	103.2

This chapter describes the preparation of TTF-TCNQ-IL composite gels for TCh detection. The composite gels TTF-TCNQ-IL combine the electrochemical properties of the TTF and TCNQ mediators with those of the ionic liquids and the resulting material displays physical properties similar to those of IL-MWCNT. Studies made using FT-IR spectroscopy showed that the mixing of the compounds lead to the formation of the TTF-TCNQ charge transfer complex and to electrostatic interaction between the mediators and the cation of the ionic liquid, and using SEM the dispersion of the TTF-TCNQ crystals in the ionic liquid was observed. Measurements in cyclic voltammetry using three types of mixtures with ionic liquids and each of the precursors showed that the TTF-TCNQ-[EMIM][TCB] gels has the highest sensitivity towards TCh. The TTF-TCNQ-[EMIM][TCB]/CP sensor was used for the development of an AChE based biosensor for the detection of carbamate drugs eserine and neostigmine.

### Selective references

- [1] T.J. Kistenmacher, T.E. Phillips, D.O. Cowan, The crystal structure of the 1:1 radical cation-radical anion salt of 2,2'-bis-1,3-dithiole (TTF) and 7,7,8,8-tetracyanoquinodimethane (TCNQ), *Acta Crystallographica Section B*, 30 (1974) 763-768.
- [7] X. Mei, J. Ouyang, Electronically and ionically conductive gels of ionic liquids and charge-transfer tetrathiafulvalene-tetracyanoquinodimethane, *Langmuir*, 27 (2011) 10953-10961.
- [13] F. Arduini, A. Cassisi, A. Amine, F. Ricci, D. Moscone, G. Palleschi, Electrocatalytic oxidation of thiocholine at chemically modified cobalt hexacyanoferrate screen-printed electrodes, *Journal of Electroanalytical Chemistry*, 626 (2009) 66-74.

## GENERAL CONCLUSIONS

In this thesis several methods were elaborated for modifying the biomolecule-transducer interface in order to obtain biosensors with improved response characteristics. PM were used as support for the immobilization of antibodies and the IL-MWCNT, MWCNT-TCNQ and TTF-TCNQ-IL composite gels with conductive properties were used as electrode materials for AChE based biosensors.

An immunosensor for OTA was developed using antibodies immobilized on PM and thiolic monolayers coupled with BSA in order to reduce non-specific interactions on the electrode surface. The PMs allowed an easy immobilization of OTA-specific antibodies and the regeneration of the electrode surface, thus obtaining a impedimetric and SPR immunosensors for OTA detection.

The detection of TCh using IL-MWCNT modified sensor was described for the first time in this. The [BMIM][BF<sub>4</sub>]-MWCNT sensor showed a high sensitivity of the TCh compared to other gels based on IL and those modified with MWCNT, and a relatively low potential for the

oxidation of TCh, and for this reason it was used in development an AChE biosensor for chlorpyrifos. For the first time the use of obidoxime for the reactivation of immobilized AChE was reported.

A method for preparing a new type of electrode material was developed using MWCNT and the mediator TCNQ. The formation of the MWCNT-TCNQ composite was confirmed by UV-Vis and Raman spectroscopy. A potential of +150 mV for the oxidation of TCh was recorded in cyclic voltammetry using a MWCNT-TCNQ modified sensor, and the sensitivity for TCh detection is six times greater for MWCNT-TCNQ/SPE then that for TCNQ/SPE. The AChE/MWCNT-TCNQ/SPE biosensor was used for the detection of methyl-paraoxon and chlorpyrifos.

In this thesis the application of TTF-TCNQ-IL composite gels in the development of sensors and biosensors was described for the first time. The TTF-TCNQ-IL gels with imidazolium cation were used in the development of TCh sensors. SEM and FT-IR studies have confirmed the formation of these composite gels. The electrochemical studies have shown that the TTF-TCNQ-[EMIM][TCB] sensor has the highest sensibility for TCh detection and it was used for the development of the AChE/TTF-TCNQ-[EMIM][TCB]/CP biosensor based on AChE for the detection of carbamate drugs.

## LIST OF PUBLISHED ARTICLES

1. Low potential thiocholine oxidation at carbon nanotube-ionic liquid gel sensor  
*Lucian Rotariu, Lucian-Gabriel Zamfir, Camelia Bala*  
Sensors & Actuators: B. Chemical, **2010**, 150, 73–79 (IF: 3.535).
2. A novel, sensitive, reusable and low potential acetylcholinesterase biosensor for chlorpyrifos based on 1-butyl-3-methylimidazolium tetrafluoroborate/multiwalled carbon nanotubes gel  
*Lucian-Gabriel Zamfir, Lucian Rotariu, Camelia Bala*  
Biosensors and Bioelectronics, **2011**, 26, 3692–3695 (IF: 5.437).
3. Highly sensitive label-free immunosensor for ochratoxin A based on functionalized magnetic nanoparticles and EIS/SPR detection  
*Lucian-Gabriel Zamfir, Irina Geana, Sondes Bourigua, Lucian Rotariu, Camelia Bala, Abdelahmide Errachid, Nicole Jaffrezic-Renault*  
Sensors and Actuators B: Chemical, **2011**, 159, 178–184 (IF: 3.535).
4. A rational design of the multiwalled carbon nanotube -7,7,8,8-tetra cyanoquinodimethane sensor for sensitive detection of acetylcholinesterase inhibitors  
*Lucian Rotariu, Lucian-Gabriel Zamfir, Camelia Bala*  
Analytica Chimica Acta, **2012**, 748, 81-88 (IF: 4.387).
5. Acetylcholinesterase biosensor for carbamate drugs based on tetrathiafulvalene-tetracyanoquinodimethane/ionic liquid conductive gels  
*Lucian-Gabriel Zamfir, Lucian Rotariu, Camelia Bala*  
Biosensors and Bioelectronics, **2013**, 46 (15), 61-67 (IF: 5.437).